International Journal of Engineering Research & Technology (IJERT)
ISSN: 2278-0181
Vol. 9 Issue 02, February-2020

Peak to Average Power Ratio Reduction in MIMO-OFDM Systems using Modified Bacterial Foraging Optimization and Iterative Learning Control

Muhammad Fawad
Department of Electrical Engineering,
University of Engineering and Technology,
Taxila, Pakistan

Muhammad Iqbal
Department of Computer Engineering,
University of Lahore,
Lahore, Pakistan

***Abstract*—Multiple Input Multiple Output (MIMO) Orthogonal Frequency Division Multiplexing (OFDM) is common and prominent technology being used for fourth generation (4G) broadband wireless communications. MIMO is combined with OFDM to obtain the benefits of both. This MIMO-OFDM technology offer resistance to frequency selective fading, tolerance from multi path delay spread, accompanied by high data rates and consistent data communication. MIMO-OFDM systems experience problem of high Peak to average power ratio (PAPR). Among methods for decreasing PAPR one is partial transmit sequence (PTS) technique. Modified bacterial foraging optimization (BFO) is used as optimization technique for rotation factors search. When this method is used in conjunction with PTS, provides less PAPR. Also, iterative learning Control (ILC) is used to decrease the PAPR. This technique provides less PAPR than BFO technique.**

***Keywords*— BFO, MIMO-OFDM, PAPR, PTS**

I. INTRODUCTION

OFDM is a multi-carrier modulation technique that has recently found wide spread application in extensive field of high data rate communication systems, including digital subscriber lines (DSL), wireless local area networks (LANs) (802.11 a/g/n) IEEE802.16, digital video broadcasting and further developing wireless broadband schemes. OFDM acceptance for high data rate use emerges mainly due to its effective and flexible control of inter symbol interference (ISI) in channels with high dispersive nature [1]. OFDM sub-carrier takes a very small bandwidth, just a few kHz, only flat fading occurs even when channel incorporates severe multipath distortions. It can be said that the OFDM can change a wide-band frequency selective fading channel into narrow-band frequency non-selective fading sub-channels. OFDM when observed in frequency domain, the frequency domain waveform or spectrum of the sub-carriers conjointly overlay i.e. fall over each other. But they do not interfere due to orthogonality among subcarriers, hence it is spectrally efficient technique [2].

Multiple transmit and multiple receive antennas (MIIMO) make use of the more propagation paths between the transmitter and the receiver. It can significantly enhance the quality of the wireless link [3]. MIMO can provide diversity gain or spatial multiplexing gain through multiple-transmit and multiple-receive antennas at high data rate. Full diversity gain can be attained for Space time block codes with two transmit antennas, or orthogonal codes for any number of transmit antennas. Decoding for these types of codes are simple due to orthogonal nature of block codes but the transmission rate is low. When same information is sent through different paths it is called diversity gain while in case of spatial multiplexing, each transmit antenna transmits different information resulting in greater transmission rate. In MIMO OFDM system, both diversity and spatial multiplexing gains can be attained but a greater diversity gain is attainable but spatial multiplexing gain reduces if diversity gain is higher (lower transmission rate) [4].

MIMO-OFDM is presently being used in 4G mobile broadband communications systems. It combines the advantages of both MIMO and OFDM. High data rates are provided with immunity to multipath propagation and spectral efficiency. But it suffers from problems of OFDM such as carrier frequency offset (CFO) caused by Doppler frequency shift, phase noise [2]and peak to average power ratio (PAPR) [5,6]. Phase noise and CFO (due to the instability of carrier signal generators used at the transmitter and receiver) degrades the performance. Doppler shift is presented by channel and produces change in frequency of the transmitter and receiver oscillator [6]. PAPR stands for peak-to-average power ratio of the transmitting signal. It is one of the major drawbacks of OFDM systems. PAPR of OFDM signals, if very high, will drive the power amplifier into the saturation region causing distortion in the signal [5]. The power amplifier must work in its linear region (i.e., with a large input back-off, where the power conversion is inefficient) to avoid distortion [7].

The methods which are used to solve the problem of PAPR are coding, tone reservation (TR), tone injection (TI), active constellation extension (ACE), clipping and filtering and amplitude clipping signal scrambling techniques such as interleaving selected mapping (SLM), partial transmit sequence (PTS), some trade-off has to be made among parameters for PAPR reduction. Parameters may be computational complexity increase, bit error rate (BER) increase, increase in transmit signal power and data rate loss [7]. This paper is organized as follows:

A brief review of MIMO-OFDM system model is presented in second section. Third section describes the PAPR in MIMO-OFDM system. Section four presents the PTS technique and section five tells briefly about bacterial foraging optimization BFO. Modified BFO for PAPR reduction is introduced in

International Journal of Engineering Research & Technology (IJERT)
ISSN: 2278-0181
Vol. 9 Issue 02, February-2020

section six. Section seven introduces the ILC for minimizing PAPR. Section eight gives discussion on simulation results.

II. MIMO-OFDM SYSTEM MODEL

MIMO-OFDM describes the MIMO system used with OFDM.

A. MIMO System

Fig.1 shows a MIMO system model with KT transmit antennas and KR receive antennas. For this system KT = KR =2. Channel is assumed to be Rayleigh fading channel. Let h_{kj} denote channel gain from kth (k=1, 2 … KT) transmit antenna to jth (j=1, 2… KR) receive antenna. The dimensions of the channel matrix H_{kj} are KT x KR.

$$H_{kj} = \begin{bmatrix} h_{11} & h_{12} \\ h_{21} & h_{22} \end{bmatrix} \quad (1)$$

B. Space-time block codes

In this system the N bits are first converted into modulated symbols $\{s'_k\}^N_{k=1}$.These symbols are space time encoded $\{s_k\}^{K_T}_{k=1}$ making a space-time codeword. k is index for antenna. The code rate for this system will be:

$$\text{Rate} = \frac{\text{Number of symbols}}{\text{Number time slots}} \quad (2)$$

Alamouti space time block code is used for two transmit antennas. Modulated symbols $\{s'_k\}^N_{k=1}$ consist of data [x_1 x_2 …x_N]. The consecutive symbols x_1 x_2 are coded as:

$$X = \begin{bmatrix} x_1 & -x_2^* \\ x_2 & x_1^* \end{bmatrix} \quad (3)$$

Equation (3) forms space-time block code. The first column contains symbols transmitted in first timeslot from antenna one and two. Similarly, second column shows symbol transmitted from antennas one and two in second time slot. During first time slot x1 and x2 are transmitted as shown in Fig. 2. In second time slot symbols are sent again in conjugate forms $-x_2^*$ transmitted from first antenna and x_1^* is transmitted from second antenna. These symbols are transmitted through channel.

C. OFDM

The discrete time OFDM symbol after inverse fast Fourier transform IFFT is:

$$x_i(n) = \frac{1}{N\sum_{k=0}^{N-1} X_i(k)e^{\frac{2j\pi kn}{N}}} \quad (4)$$

N= number of subcarriers, Where, k= [0, 1, 2…N-1],$1 \le i \le$ KTn=index of symbol x_i signal in discrete time domain andX_i =signal in frequency domain.MIMO-OFDM system is formed by passing data bit through Alamouti encoder, which is then passed through OFDM block. The system diagram is shown in Fig. 3.

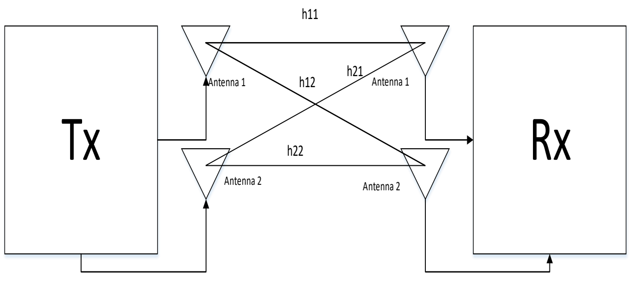

Figure 1. Block diagram of MIMO system

D. PAPR in MIMO-OFDM System

Due to additive nature of IFFT subcarrier components of OFDM modulated signal are added thus giving high peaks and producing the issue of PAPR. When the input of the linear amplifier is more than the normal operating value of amplifier then a non-linear distortion occurs at the output because the signal goes into the saturation region of amplifier which makes the output nonlinear. It causes out of band radiation which disturbs the signals in adjacent band. In band distortion cause rotation attenuation and offset of the signal [7]. Fig. 3 shows system diagram for PAPR in MIMO-OFDM system.

PAPR of signal x (n) is defined as in eq. 5:

$$\text{PAPR} = \frac{\max|x(n)|^2}{\text{mean } |x(n)|^2} \quad (5)$$

The PAPR is observed in terms of complementary commutative distribution function (CCDF). CCDF for K_T transmit antennas is given by (6)-(10).

$$\text{CCDF}=1-\text{CDF} \quad (6)$$
$$\text{CCDF}=\Pr(\text{PAPR}>\text{PAPR}_0) \quad (7)$$
$$=1-\Pr(\text{PAPR}<\text{PAPR}_0) \quad (8)$$
$$= 1 - F(\text{PAPR}_0)^{K_T N} \quad (9)$$
$$= 1 - (1 - e^{-\text{PAPR}_0})^{K_T N} \quad (10)$$

In MIMO-OFDM system, the PAPR is the maximum PAPR value of the $K_T$transmit antennas[1].

$$\text{PAPR} = \max_{1 \le i \le KT} (\text{PAPR}_i) \quad (11)$$

E. Partial Transmit Sequence in MIMO-OFDM System

PTS is applied separately at each transmit antenna. The Alamouti coded data after passing through OFDM block is converted into partial transmit sequences. Suppose two data streams to be sent from two antennas are $\mathbf{X_1}$ and $\mathbf{X_2}$containing complex entries. These data blocks are converted into P disjoint subblocks expressed by (12) [5].

$$\mathbf{X_1} = [\mathbf{X_1^1 X_1^2 X_1^3} \ldots \mathbf{X_1^P}]^T \quad (12)$$

All the subblocks have same size and data do not overlap. Subblocks of same size are made by appending zeros at places where no data is present. If all these subblocks are summed the original signal $\boldsymbol{X_1}$ will be formed.$\mathbf{X_1} = \sum_{p=1}^{P} X^P$. Each subblock is rotated by a different phase factor W. Terms phase factors and phase vectors are used interchangeably. A total of P phase factors are used while value of allowed phase factors is W.

$$b^p = e^{j\varphi p} \text{where p=1, 2, 3….P} \quad (13)$$

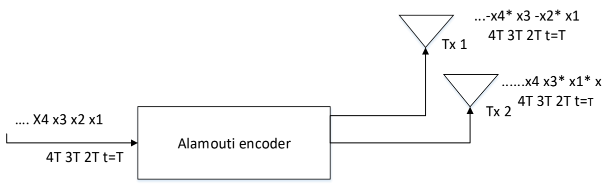

Figure 2. Block diagram for Alamouti encoder

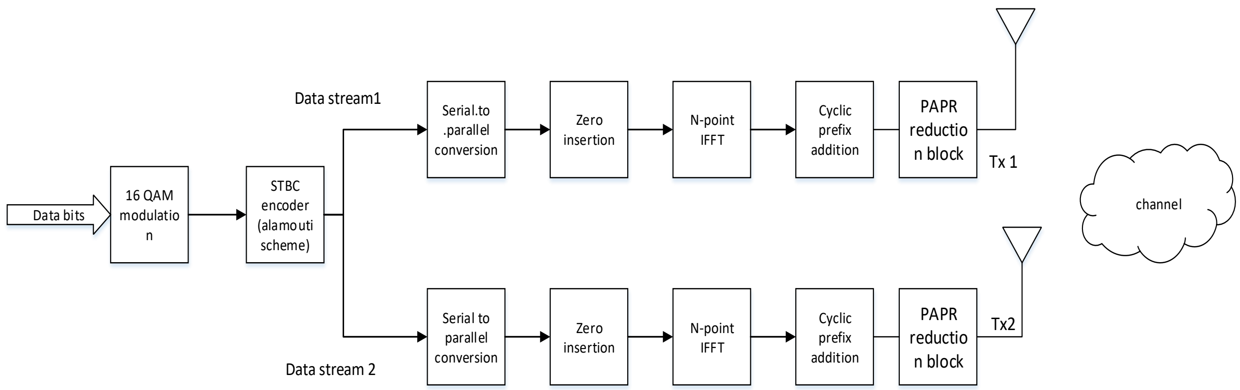

Figure 3. Block diagram for MIMO-OFDM system model with PAPR reduction block

Equation (13) tells b^p is phase factor. Then, the subblocks are changed into P time-domain partial transmit sequences by taking their IFFT as given in (14).

$$\mathbf{x} = \mathrm{IFFT}\{\sum_{p=1}^{P} b^p \mathbf{X^p}\} \qquad (14)$$

These IFFT can also be taken before multiplying the data blocks with phase factors. The above expression in (14) and the one given below in (15) both are equivalent expressions.

$$x = \sum_{p=1}^{P} b^p . \mathrm{IFFT}\{\mathbf{X^p}\} \qquad (15)$$

$$x = \sum_{p=1}^{P} b^p \mathbf{x^p} \ (16)$$

$\{\mathbf{x^p}\}$ is the time domain partial transmit sequence.

The objective has been to optimally combine the P subblocks to obtain the time domain MIMO-OFDM signals with the lowest PAPR. The PTS technique reduces the PAPR, but finding optimal phase factors is very complex. Optimal phase factors are optimized by (17).

$$[\tilde{b}^1, \ldots \tilde{b}^P] = \arg\min_{[b1,\ldots bP]} \left(\max_{n=0,1,\ldots N-1} \left| \sum_{p=1}^{P} b^p x^p [n] \right| \right) \qquad (17)$$

The signal with lowest PAPR is given by (18).

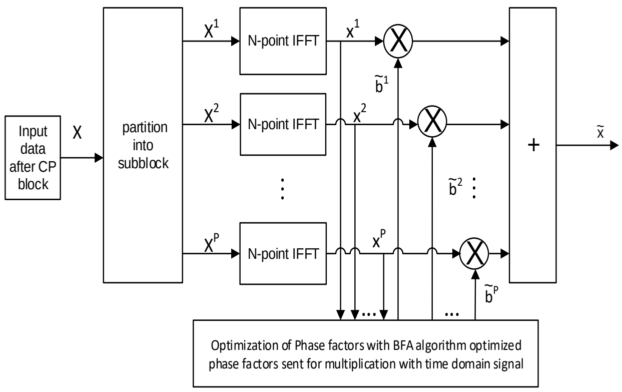

Figure 4. Block diagram for PTS scheme for PAPR reduction (PAPR reduction block)

$$\tilde{\mathbf{x}} = \sum_{p=1}^{P} \tilde{b}^p \mathbf{x^p} \qquad (18)$$

Only small number of phase factors i.e.$\{b^p\}_{p=1}^{P}$ are chosen to keep complexity in check. Phase factors set is b= $\{e^{j2\pi i/W} | \ i=0, 1\ldots W-1\}$, W^{P-1} sets of phase factors are tested to find the optimum set. So, the search complexity increases exponentially as number of subblocks increase [7].

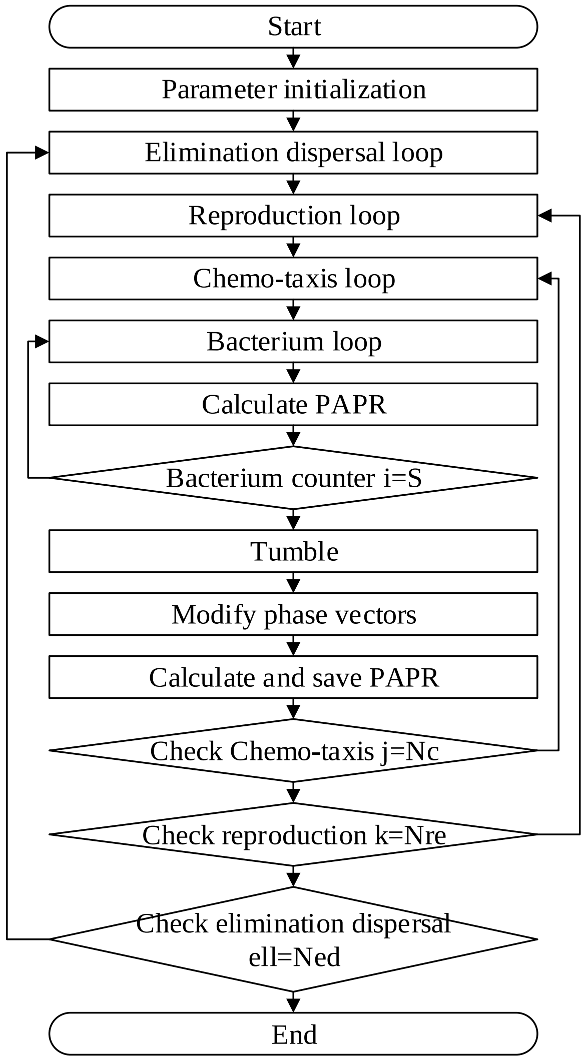

Figure 5. Flow chart for PTS with BFO

F. Bacterial Foraging Optimization

BFO is the latest biologically stimulated optimization procedure. It copies the food hunting movement of E. coli bacteria for optimization process. E. coli is the bacteria found in human intestines. Bacterial food hunting or bacterial for aging process was proposed as an effective optimization process in [8] where it was used to optimize distributed controller. It has also been used in optimal power flow [9]. The foraging process of bacteria is a [8]:

- Chemo-taxis
- Reproduction
- Elimination and Dispersal

The most important step of foraging actions of E. coli bacteria is Chemo-taxis. In this process bacteria tumbles initially (movement in a random direction) and checks the concentration offood materials and if suitable concentration present, it swims in same direction thus maximizing the quantity of nutrients at the completion of foraging. Swim is also in form of directed steps. Concentration of food is checked after each swim. Swim continues if concentration of food is increasing. Every bacteria of population performs chemo-taxis. The process is applied on whole amount of bacteria in population. On basis of food collected, some bacteria get eliminated rest of them bacteria divide, keeping the population constant.

G. Partial Transmit Sequence with Modified Bacterial Foraging Optimization

BFO is being adopted to optimize PAPR of MIMO-OFDM data. Optimized phase vectors are obtained through BFO. The search space in this algorithm comprises of bacteria. The phase vectors are the search space. Bacteria search for the optimal solution. Each bacterium undergoes several steps before giving optimal solution. The objective function is the PAPR, that is optimized. Multidimensional matrices hold the data as well as the randomly generated phase vectors. Data and phase vector matrices multiply to give PAPR and form the solution space. The solution space has Nsbsubblocks and W phase vectors. This data is coming from OFDM sub-block where it is passing through serial to parallel converter. After serial to parallel conversion zeros are appended and IFFT is taken to produce sub-block data. These sub blocks are processed through BFA block to optimize phase vectors for optimum PAPR. Inside BFA block parameters are first initialized. Main parameters of BFO block are bacterium counter, chemotaxis counter reproduction counter and elimination and dispersion counters. Main parameters of data or test system are data stream memory, PAPR vector; tumble vector, phase vectors, data bits and chemo-taxis step size. This algorithm works in four successive loops. These can be divided as inner loops and outer loops. Two inner loops and two outer loops are present. Inner loops contain main functionality of this algorithm. Inner loops consist of bacterium and chemotaxis counters. PAPR is calculated in chemotaxis counter. In chemotaxis counter successive tumbles occur and modify phase vectors to calculate PAPR. Outer loops consist of reproduction and elimination/dispersal counters. Inner loops repeat in outer loops. As larger number of data combinations is being searched in case of probability of elimination dispersal i.e. Ped=1

H. Modified Bacterial Foraging Optimization Algorithm

Step 1:Initialize BFO Parameters

S// Amount of bacteria
Nc// Chemo-taxis steps
Nre// Number of reproduction
Ned// Number of elimination-dispersal loops

PTS System parameters

All V// Phase vectors
D// Data for subblocks
DS// Data stream formed by multiplication of phase vectors and subblocks
PAPR// PAPR
DEL// for phase vectors generated randomly
//Initialization of events loop

Step-2

ell=ell+1 // Elimination/dispersal loop

Step-3

k=k+1 // Reproduction loop

Step-4

j=j+1// Chemo-taxis loop
//Start Chemo-taxis and bacterium counter
For i=1,2,…S

Step 5

Evaluate the PAPR and save
If i=S → end bacterium counter
Perform tumble by Generating DEL randomly

Step 6

Modify phase vectors by V=VxDEL
Calculate and save new PAPR
If j=Nc end chemotaxis loop start next reproduction else continue chemotaxis.
If k=Nre end reproduction and start elimination dispersal
If ell=Ned end loop

Step 7

Find minimum of all PAPR stored.

Three main modifications are done in this algorithm. Swim and swarming is excluded. Swarming is excluded because this algorithm is using very small number of bacteria. Furthermore, swarming is main tool to provide diversity in search space but here in this algorithm being proposed, randomly generated vector in chemotaxis is filled with search space options to gain diversity so swarming is rather excluded to have computational benefits in algorithm. Swim provides very small change in values of PAPR making the search very complex. Swim is compensated by using larger number of tumbles in chemo-taxis. Using delta vector in search space in chemotaxis to mimic tumble can provide alternate efficient and reliable method instead of swim. Next the reproduction step is simplified by keeping the population of previous generation same while obtaining entirely new population in new generation instead of retaining better half of previous population. Elimination dispersal is performed with a probability of Ped=1. Which mean all new bacteria are used in new elimination dispersal event, while keeping previous data stored. The motivation for these steps is that the combination search for optimum phase factors requires to find best combination among all possible combinations. So greater the combinations, greater will be the possibility of finding best solution. Generating new population randomly in reproduction and eliminating whole population and using new one for next elimination dispersal event gives the opportunity to obtain maximum possible combinations.

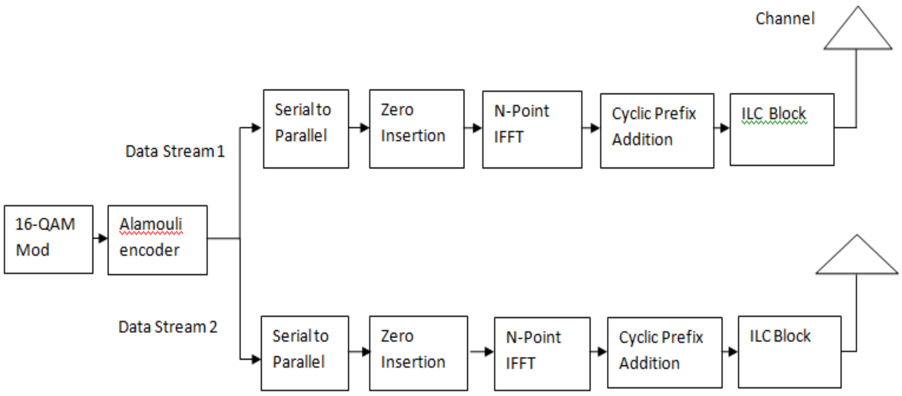

Figure 6. Block diagram of PARP reduction using ILC

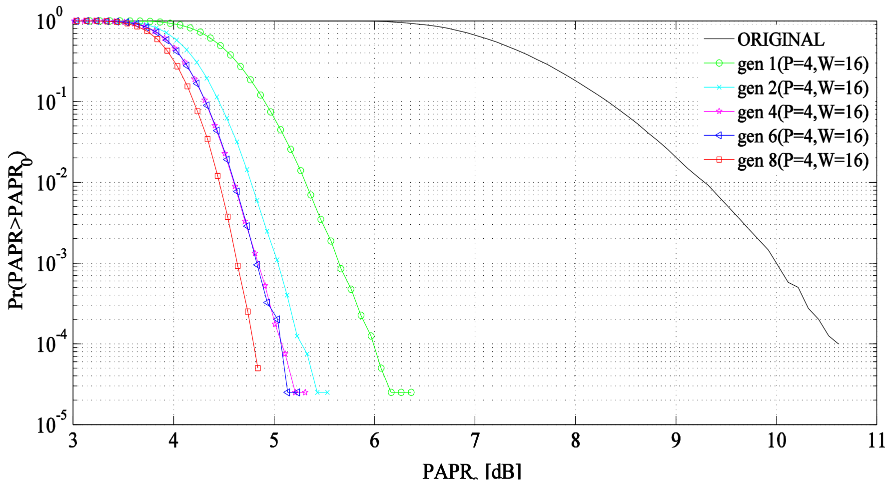

Figure 7. CCDF for different generations P=4 and W=16

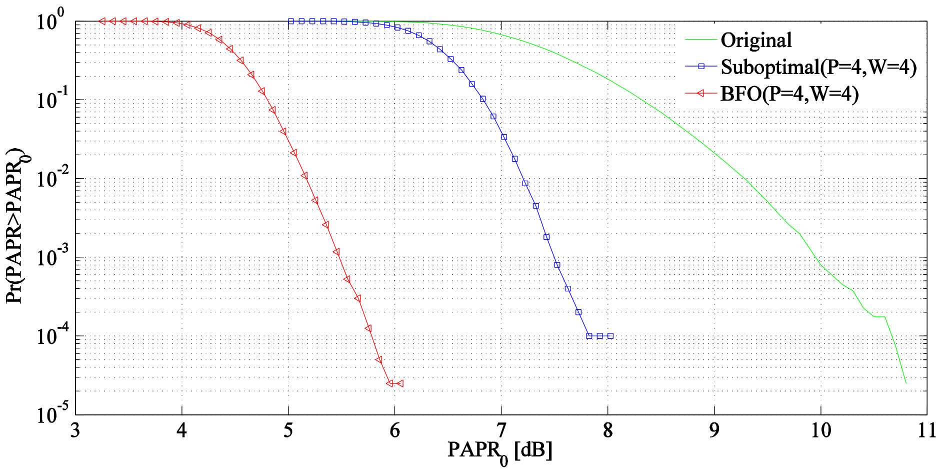

Figure 8. CCDF for original, suboptimal and BFO, P=4 and W=4

Flow chart for this algorithm is shown in Fig.5.

I. PAPR Reduction using ILC

For designing ILC, few assumptions are made so that the process of learning can be improved from previous learning mechanism. These assumptions are mentioned in ILC work [11-14]. The starting point of every iteration will always remain the same, which is if system starts from t=0 having a magnitude of zero as initial condition then all the trails must begin will the same initial condition all the time. The error should be converged after each iteration which is the error of second trail must be less than the error of first trail and so on. The time for each iteration should be the same, which is, if first trail was of duration 10 sec than all other trails will also have the same time. These assumptions must be followed in order to track the system perfectly. There are different updates law for designing

International Journal of Engineering Research & Technology (IJERT)
ISSN: 2278-0181
Vol. 9 Issue 02, February-2020

of ILC. Different scholars have used different ways to design ILC. Some of the most important forms of ILC are discussed below. The most common and general form of ILC is D type ILC. In this scheme derivative of error is applied to generate a new control signal through iteration [15]. The mathematical form of D-ILC is given by:

$$u(i,k+1) = u(i,k) + K\dot{e}(i,k)$$

Where $\dot{e}(i,k) = \dot{y}(i) - \dot{y}(i,k)$the error on which a derivative operation is performed, K is the gain matrix that specifies how much weightage user wants to give to an error signal. The error at the first iteration is zero because the initial condition is same for all iterations.

The classical calculation of the Iterative Learning Control problem is, given a reference trajectory and a system, find (using an iterative procedure) the input to the system such that the output follows the desired trajectory as well as possible. $K$is the number of trial. During the k^{th}trial an input u_k is applied to the system producing the output y_k. These signals are stored in the memory units until the trial is over. The error is calculated between the actual output and desired output as $E_{k=}y_d - y_k$. Where y_d is the reference PAPR and y_k is the Current PAPR at iteration k, Based on this error ILC algorithm computes a modified input signal u_{k+1} , that will store in memory unit. The next time this new input signal is applied to the system. This new input signal is designed as to produce a smaller error than the previous one. The iteration is repeated as many time as defined by the user. This is implemented to reduce PAPR and gives the following result, in which the PAPR is reduced from 10 dB to 1 dB.

III. SIMULATION RESULTS

The simulation results are obtained by using W=2, 4, 8 and 16 phase vectors and P=2, 4, 8 and 16 subblocks. P is the subblocks while W is the phase vectors. Phase vectors are used from set of {±1, ±j, ±0.707±j0.707, ±0.577±j0.577}. 16-QAM modulation and N=256 subcarriers are used. PAPR is calculated for 10,000 symbols. The oversampling factor L is kept 4. Simulations are done for various combination of phase factors with different number of subblocks. The parameters for modified BFO are Nre, Ned, Nc and S. Summary of parameters is shown in Table 1 and Table 2. Table 3 shows the complexity of modified BFO. Table 4 shows results in tabulated form.

Fig 7 shows different generations for BFO give PAPR reduction. Simulations show that with P=4 and W=16 generation 8 gives the best results. As the number of generations is increased the PAPR performance becomes better. For all other simulation the results are obtained for generation 8. The original PAPR calculated is 10.62 dB for generation 1 PAPR reduces to 6.36 dB for generation 2 PAPR reduces to 5.53 dB gen 4 gives PAPR reduction of 5.31 dB and gen 6 gives PAPR reduction of 5.23 dB. Finally, the gen 8 gives best results of 4.83 dB. Generation 8 has 1.53 dB improvement compared to gen 1. 5.79 dB improvement is shown compared to original signal.

Fig 8 shows a comparison of BFO with suboptimal method and original signal. When W=4 and P=4 the PAPR reduces to 6.05 dB with the application of BFO from original PAPR of 10.8 dB. The same phase vectors and subblocks used for suboptimal method reduces PAPR to 8.02 dB. Suboptimal method shows 2.78 dB improvement while BFO shows 4.75 dB improvement compared to original signal.

Fig 9 shows comparison of different phase vectors while keeping the subblocks same. As more number of phase vectors are used by keeping the subblocks constant slight improvement in PAPR is shown. When P=8 while W=2, 4, 8 and 16 phase vectors are used. For W=16 the PAPR reduces from 11 dB to 4.91 dB. For W=8, 4.88 dB and W=4 PAPR reduction is 5.08 dB. For W=2 PAPR reduces to 5.05 dB. The least PAPR gain achieved is 5.95 dB.

Fig 10 shows CCDF when different subblocks are used and phase factors are kept same=2 phase vectors are used. For different subblocks P=2, 4, 8 and 16 and W=2, original PAPR is 10.67 dB. For P=2 PAPR is 9.9 dB P=4, 8 and 16 PAPR is 7.1 dB, 5.03 dB and 4.78 dB respectively. Overall 5.89 dB PAPR is reduced. Least PAPR reduction is 0.77 dB achieved by P=2.

Fig 11 shows comparison of PAPR using ILC and without using ILC and BFO. The PAPR gain achieved using ILC is 1 dB, on the other hand the PAPR gain without ILC and BFO is 10 dB. The PAPR gain using ILC shows better result as compared to previously discussed techniques.

TABLE 1: Simulations Parameters used for MIMO-OFDM system and PTS

Parameter name	Value
Oversampling factor	L=4
Carriers	256
Modulation	16-QAM
Phase vectors used	{±1, ±j, ±0.707±j0.707, ±0.577±j0.577}.
Number of subblocks	2,4,8,16

TABLE 2: Parameters used for BFO

Parameter name	Symbol
Number of bacteria	S
Chemotaxis steps	Nc
Reproduction events	Nre
Elimination dispersal steps	ell

TABLE 3: Computational complexity comparison of OPTS, BFO and modified BFO

Method	Computational complexity
OPTS [10]	W^{P-1}
BFO [10]	N*Nc*Ns
Modified BFO	ell*Nre*Nc*S

TABLE 4: PAPR for Subblocks and different phase vectors

Combinations	PAPR (dB)	PAPR (dB) [10]
P=4, W=16	4.83	6.3
P=8, W=2	5.05	6.5
P=8, W=4	5.08	5.6
P=8, W=8	4.88	-
P=8, W=16	4.91	-
P=2, W=2	9.9	9.8
P=16, W=2	4.45	5.8

International Journal of Engineering Research & Technology (IJERT)
ISSN: 2278-0181
Vol. 9 Issue 02, February-2020

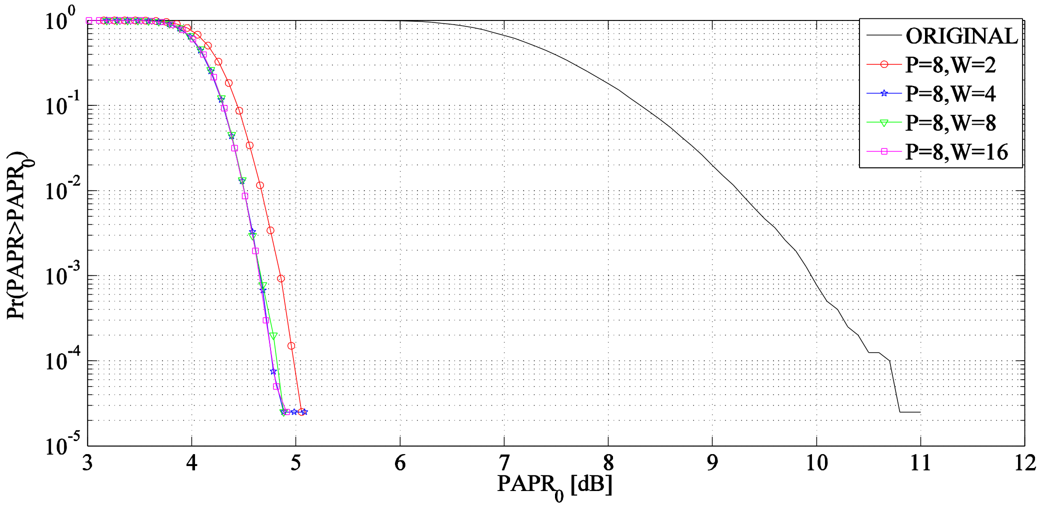

Figure 9. CCDF for different phase vectors with, P=8 sub blocks

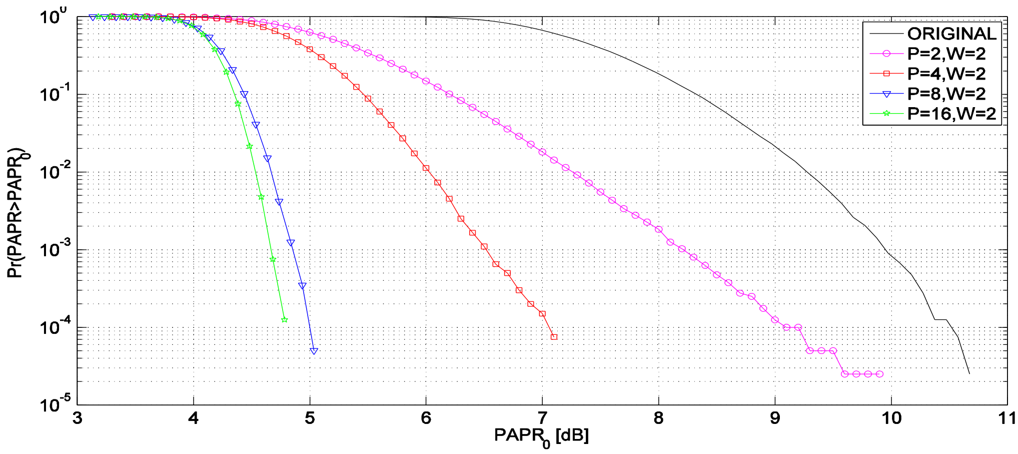

Figure 10. CCDF for different subblocks and W=2 phase vectors

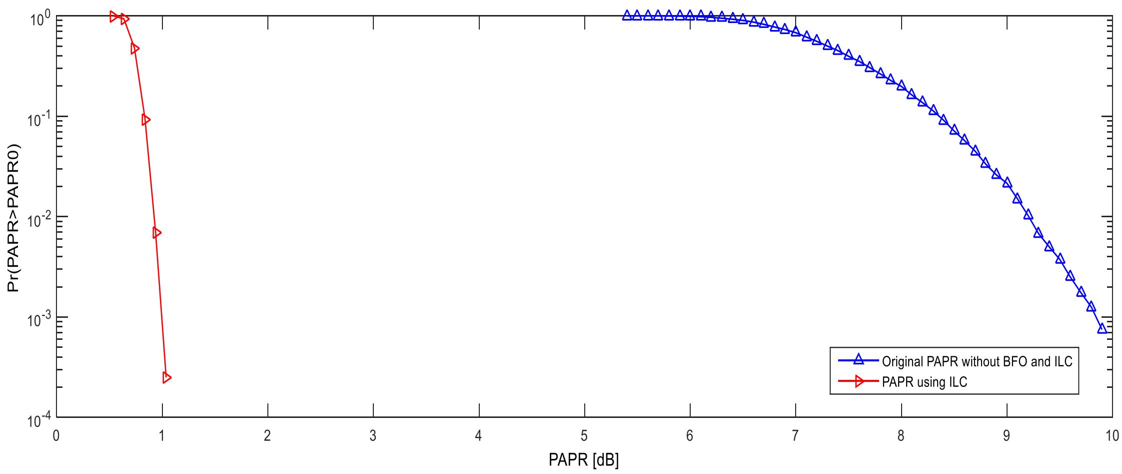

Figure 11. Comparison of PAPR using ILC and PAPR without BFO and ILC

IV. CONCLUSIONS

The PAPR is reduced by both techniques, Modified Bacterial Foraging Optimization and Iterative Learning Control. The modified bacterial foraging optimization shows the best results at P=4, W=16 and generation 8, in which PAPR reduces from 11 dB to 4.91dB. The Iterative Learning Control gave best result as it reduced the PAPR from 10 dB to 1dB.The

International Journal of Engineering Research & Technology (IJERT)
ISSN: 2278-0181
Vol. 9 Issue 02, February-2020

both techniques can be used in MIMO-OFDM system, as well as, with some modification, can be applied for SISO-OFDM systems.

REFERENCES

[1] D. Phetsomphou, S. Yoshizawa, Y. Miyanaga(10th International Symposium on Communications and Information Technologies, Japan, IEEE, 2010).
[2] Y. Wu, W. Y. Zou, IEEE Transactions on Consumer Electronics, 41 (1995) 392.
[3] Z. Safar, K. J. R. Liu(11th European Signal Processing Conference, IEEE, France, 2002).
[4] K. H. M. and B. C. Levy (Topical Conference on Wireless Communication Technology, 2003).
[5] Cho, Y. Soo, J. Kim, W. Y. Yang, C. G. Kang (Asia: Wiley & Sons, 2010).
[6] M. Hasan, S. P. Majumder (IEEE Second International Conference on Communication Software and Networks, ICCSN'10,2010).
[7] S. H. Han and J. H. Lee (Wireless Communications, IEEE, 12, 56-65, April 2005).
[8] Passino and K. M (Control Systems, IEEE, vol. 22, no. 3, pp. 52-67, 2002).
[9] Tang, W. J., Q. H. Wu and J. R. Saunders (IEEE Congress on Evolutionary Computation (CEC 2006), 2006).
[10] M. S. R. Manjith(Research Journal of Applied Sciences, Engineering and Technology, vol. 7(21), pp. 4423-4433, 2014).
[11] Yang Quan Chen and Kevin L. Moore (Proceedings of the American Control Conference Anchorage, AK May 8-1 0,2002).
[12] Rogers, Galkowski, and D.H. Owens (ISBN-13: 978-3540426639,Springer 2007).
[13] Bristow, Tharayil, and Alleyne (IEEE, 26(3): p. 96114, 2006).
[14] Younging Wang., FurongGao, and Francis J. Doyle (Journal of Process Control, Elsevier, 2009. 19(10): p. 1589-1600).
[15] H. S. Ahn, Y. Chen and K. L. Moore, IEEE Transactions on Systems, Man, and Cybernetics, Part C (Applications and Reviews), vol. 37, no. 6, pp. 1099-1121, Nov. 2007.